SciEn
Journal of Engineering Advancements Vol. 07(03) 2026, pp 125-132 https://doi.org/10.38032/jea.2026.03.003

Comparative Numerical Analysis of Thermal Performance in Modified Horizontal U-Tube Ground Heat Exchanger

*Jyothy Mondal, Plaban Rudra Paul, Md. Hasan Ali**

Department of Energy Science and Engineering, Khulna University of Engineering & Technology, Khulna-9203, Bangladesh

Received: January 13, 2026, Revised: September 21, 2026, Accepted: September 22, 2026, Available Online: October 04, 2026

ABSTRACT

Geothermal energy stands out as a reliable and sustainable solution for heating and cooling buildings, delivering consistent baseload power unaffected by weather or geopolitical factors. Moreover, its subtle design blends seamlessly with the surroundings. This research evaluates the thermal performance of horizontal ground heat exchangers (GHEs), comparing around 17 configurations. A trench with dimensions of 28 m × 3 m × 5 m was modeled, maintaining uniform trench and pipe lengths of 18.35 m and 37 m, respectively, for all configurations. ANSYS FLUENT was used to simulate a 72-hour continuous cooling operation where water was circulated at 2 L/min with an inlet temperature of 303 K, while the soil's initial temperature was 290 K. A time-step size of 60 s was used, with convergence achieved when the energy-equation residuals fell below 10^{-6}. After 72 hours of operation, C10 (inner diameters 40.0/61.6 mm and outer diameters 48.0/69.6 mm) and C16 (inner diameters 45.0/55.9 mm and outer diameters 53.0/63.9 mm) reached similar outlet temperatures, with C16's average heat transfer rate being marginally lower than that of C10, a difference small enough to be disregarded. Furthermore, the average heat transfer rates per meter trench for C10 and C16 were 38.17 W/m and 38.15 W/m, respectively, indicating effective space utilization and cost efficiency. Additionally, this configuration demonstrated superior thermal performance compared to other modified designs, requiring less pumping power due to reduced pressure loss. Increasing the flow rate from 0.5 to 2 L/min increased the average heat-transfer rate from 378.62 to 700.48 W, representing an 85.01% improvement, although the gain decreased at higher flow rates. Among the investigated pipe materials, HDPE achieved the highest heat-transfer rate of 815.57 W, 16.43% higher than PVC. For the investigated ground materials, sand provided the highest heat-transfer rate of 892.88 W, 27.47% higher than clay. Though U-tubes are generally efficient, diameter-optimized configurations can offer better performance for practical applications.

Keywords: Geothermal energy, Thermal performance, Horizontal Ground Heat Exchanger, Modified U-tube

Copyright @ All authors

This work is licensed under a Creative Commons Attribution-Non Commercial 4.0 International License.

1 Introduction

Energy is the lifeblood of today's modern world, powering everything from homes to industries. Most of the world's energy relies on fossil fuel sources that require millions of years to form. Over 80% of global energy needs are met by fossil fuels. That is why continuation of the current usage rate could deplete coal and natural gas by 2060. Despite various strategies to lessen reliance on these fuels, global energy consumption is still on the rise, but the consequences of intensive fossil fuel usage have started to be acknowledged due to its scarcity and the risk of contamination of existing fossil fuel resources. As a result, human beings started seeking alternative sources of energy that can be replenished swiftly by natural processes, thereby reducing pollution and offering a sustainable energy solution over extended periods. Many renewable energy sources, such as solar, wind, hydropower, ocean energy, bioenergy, and geothermal energy, can provide an effective means of powering industries with negligible CO_2 emissions, serving as a cleaner alternative to oil, coal, and gas [1],[2]. The rapid expansion of solar and wind energy has strengthened global efforts to reduce greenhouse gas emissions and accelerate the transition toward renewable energy [3]. Geothermal energy is becoming more popular due to its consistency, reliability, availability, energy efficiency, economic benefits, and geographical suitability, along with technological advancements. Due to its accessibility in extracting heat from the Earth's crust it is rising as an important and complementary source [4]. This heat can be directly used for heating or converted into electricity through steam generation. Beyond electricity generation, geothermal energy can be utilized for multiple purposes, including heating buildings, supplying district heat, warming water, and powering industrial processes. GSHPs harness the stable temperatures through a ground heat exchanger (GHE) installed in either horizontal trenches or vertical boreholes to provide heating and cooling for domestic purposes [5],[6]. Horizontal GHEs form a closed loop with a circulating heat transfer fluid placed in shallow trenches, typically 1–2 meters deep below the surface. Pipes are then placed in these trenches in straight runs or a coiled pattern to increase surface area. This installation method is less complicated than vertical installations as it avoids the need for specialized drilling equipment. Hence, for small buildings, horizontal GHEs are often chosen. Although they provide benefits in installation and cost, their performance is affected by several factors such as soil conditions, design and layout of GHE, along with thermal properties of fluid [7],[8].

In recent times, new configurations of horizontal GHEs have been introduced to enhance heat transfer efficiency, including

*Corresponding Author Email Address: hasan@ese.kuet.ac.bd Published by: SciEn Publishing Group

serpentine, spiral, double U-tube, etc., gaining popularity for their superior features over traditional designs. Extensive research has been conducted by engineers and researchers to optimize the design of new patterns and structures [9]. Florides and Kalogirou's [10] review various GHE models and their practical applications. In the case of horizontal GHEs, they recommend installation at depths ranging from 1.5 to 2 meters. To minimize interference between pipes, a separation of 30 cm is advised, with trenches spaced at least 2 meters apart. Moreover, Badescu [11] designed a simple and precise GHE model comprising a single 36-meter tube buried under three different soil types: bare soil, short-grass-covered soil, and asphalt-covered soil. Additionally, various pipe materials, including PVC, steel, plastic, aluminum, concrete, and rough-cast, were considered, but their impact on heating and cooling energy was minimal. On the other hand, Benazza et al. [12] research focused on a configuration of 8 concentric tubes, each with a diameter of 0.03 meters, spaced 0.7 meters apart over a 5.64-meter radius, and buried 2.5 meters deep, representing a horizontal circular heat exchanger covering 100 m². They analyzed the effects of thermal conductivities and geometric parameters on the heat exchanger's efficiency, finding that decreasing the spacing between tubes increases the heat flux per square meter, although the increase is not directly proportional to the length of the tubes. Additionally, Esen et al. [13] set up a single-pass straight tube GHE at the University of Firat, featuring a 16mm diameter high-density polyethylene tube buried at a depth of 1 meter in the natural soil. Their numerical and experimental results showed a good correlation, with an average difference of about 0.6°C. Furthermore, Adamovsky et al. [14] focused on analyzing soil temperature, heat flows, and the energy transferred from the soil using two types of horizontal GHEs: a linear heat exchanger and a slinky-type heat exchanger. Results indicated that the linear heat exchanger is more effective as a low-grade power source for heat pumps. A numerical investigation by Jahan et al. [15] numerically examined the performance of horizontal U-tube, spiral, and slinky GHEs during 7 days of cooling operation. Their analysis showed that the slinky GHE exhibited the best thermal efficiency, achieving a heat exchange rate of 20.72 W/m. In comparison, the U-tube and spiral configurations achieved 9.75 W/m and 13.62 W/m, respectively, meaning the slinky design provided 53% and 28% higher heat transfer than the U-tube. Despite its superior heat exchange rate, the slinky configuration also experienced the highest pressure drop, reaching up to 87% above the U-tube system. Hu et al. [16] conducted a numerical energy balance analysis to compare three horizontal GHE layouts over a one-year operational period. Their results indicated that the linear configuration performed the best, offering faster simulations, simpler geometry, and less sensitivity to environmental influences. Spiral and slinky designs demand a more optimal configuration due to coil interactions and higher dependence on external conditions. Hossain et al. [17] carried out simulations and field studies in Joypurhat, Bangladesh, to examine the effectiveness of an earth water pipe heat exchanger (EWPHE) system during the coldest month, January. They identified 3.5 m burial depth and 50 m pipe length as optimal for lowering the temperature from 35 °C to 27 °C. Their analysis showed minimal variation across GI, Steel, PVC, and HDPE pipes but a decline in performance with increased flow rate. Field experiments achieved an efficiency of 55%, demonstrating strong potential for practical use in Bangladesh.

Research on horizontal GHEs centered on geometry-based variations (serpentine, slinky, spiral, helical), along with material, depth, and working-fluid optimization. However, comparatively limited attention has been given to modifying the diameter of a horizontal U-tube along its flow path as a means of simultaneously influencing heat transfer and hydraulic performance. Therefore, a modified horizontal U-tube GHE consisting of a differential tube diameter will be employed in this research to improve the thermal output as compared to a conventional horizontal U-tube system. Seventeen configurations were developed where the surface area will be kept constant across both the conventional and modified designs. By conducting simulations using ANSYS FLUENT software for various modified designs and comparing their outlet temperature, heat-transfer rate and pressure drop, the configuration with the most favorable thermal-hydraulic performance will be identified, and experimental performance will be evaluated.

2 Methodology

ANSYS Fluent was employed to perform CFD-based simulations analyzing fluid flow and heat transfer in the GHE system. The developed numerical model investigates various GHE configurations during cooling operation over 72 hours, with a focus on thermal performance comparison. Several geometric and operational parameters, including tube diameter, installation depth, flow rate, ground and pipe material, were modified.

2.1 Description of the Geometric Model

The geometric configuration of the modified U-tube horizontal GHE, incorporating two different pipe diameters at specific positions along the total pipe length, creating a divergence at the joint, is illustrated in Fig. 1. The pipe diameters are defined by DH1, DL1, DH2, and DL2, which represent the diameters of the respective pipe sections before and after the diameter divergence. The corresponding pipe lengths are denoted by H1, L1, H2, and L2, describing the lengths of each section along the flow path, while trench length and spacing between pipes are represented by 18.35 m and 0.3 m, respectively. These parameters will be varied during simulations to identify the optimal design of the modified U-tube. To enable consistent comparison across models, pipe diameters were systematically varied while maintaining constant material volume and outer surface area. As the diameter increased, the outer surface area rose proportionally due to its dependence on circumferential length, whereas the material volume was the difference between the inner and outer diameters. A detailed summary of the geometric characteristics, along with the diameter-dependent variations in outer surface area and material volume for each GHE configuration, is presented in Table 1.

All models were embedded in a clay trench measuring 28 m in length, 5 m in depth, and 3 m in width, with water used as

the circulating fluid. A uniform burial depth of 1.5 m and a wall thickness of 0.004 m were maintained across all designs. In addition to polyvinyl chloride (PVC), low-density polyethylene (LDPE), HDPE, and polyethylene (PE) pipes were investigated to evaluate their thermal performance, with similar assessments carried out for various soil materials. Furthermore, this research explored the influence of different flow rates on heat transfer efficiency. Table 2 outlines the necessary thermophysical properties of the materials.

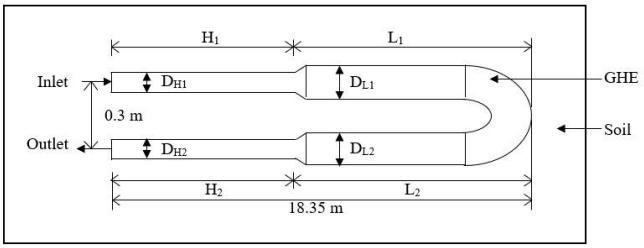

Fig. 1 Schematic diagram of modified horizontal U-tube GHE

Table 1 Geometric characteristics of different GHE configurations

Configurations	Length (m)				Diameter (mm)					Depth (m)	Outer Surface Area (m^2)	Material Volume (m^3)
	H1	L1	H2	L2		DH1	DH2	DL1	DL2			
C1	8.5	10	8.5	10	Inner	25.4	25.4	25.4	25.4	1.5	3.19	0.020
					Outer	33.4	33.4	33.4	33.4			
C2	8.5	10	8.5	10	Inner	50.8	50.8	50.8	50.8		6.38	0.081
					Outer	58.8	58.8	58.8	58.8			
C3	8.5	10	8.5	10	Inner	25.4	25.4	50.8	50.8		4.79	0.051
					Outer	33.4	33.4	58.8	58.8			
C4	18.5	0	18.5	0	Inlet	25.4	50.8	N/A	N/A			
					Outlet	33.4	58.8	N/A	N/A			
C5	18.5	0	18.5	0	Inlet	50.8	25.4	N/A	N/A			
					Outlet	58.8	33.4	N/A	N/A			
C6	18.5	0	18.5	0	Inner	25.4	76.2	N/A	N/A		6.38	0.101
					Outer	33.4	84.2	N/A	N/A			
C7	18.5	0	18.5	0	Inner	76.2	25.4	N/A	N/A			
					Outer	84.2	33.4	N/A	N/A			
C8	18.5	0	18.5	0	Inner	30.0	71.6	N/A	N/A			0.095
					Outer	38.0	79.6	N/A	N/A			
C9	18.5	0	18.5	0	Inner	71.6	30.0	N/A	N/A			
					Outer	79.6	38.0	N/A	N/A			
C10	18.5	0	18.5	0	Inner	40.0	61.6	N/A	N/A			0.085
					Outer	48.0	69.6	N/A	N/A			
C11	18.5	0	18.5	0	Inner	61.6	40.0	N/A	N/A			
					Outer	69.6	48.0	N/A	N/A			
C12	18.5	0	18.5	0	Inner	40.0	59.6	N/A	N/A		6.26	0.081
					Outer	48.0	67.6	N/A	N/A			
C13	18.5	0	18.5	0	Inner	59.6	40.0	N/A	N/A			
					Outer	67.6	48.0	N/A	N/A			
C14	18.5	0	18.5	0	Inner	35.0	62.7	N/A	N/A		6.14	
					Outer	43.0	70.7	N/A	N/A			
C15	18.5	0	18.5	0	Inner	62.7	35.0	N/A	N/A			
					Outer	70.7	43.0	N/A	N/A			
C16	18.5	0	18.5	0	Inner	45.0	55.9	N/A	N/A		6.34	
					Outer	53.0	63.9	N/A	N/A			
C17	18.5	0	18.5	0	Inner	55.9	45.0	N/A	N/A			
					Outer	63.9	53.0	N/A	N/A			

Table 2 Thermophysical characteristics of various materials

Materials	Types	Parameters		
		Thermal Conductivity, k (W/mK)	Specific Heat, Cp (J/kg K)	Density, ρ (kg/m^3)
Tube	HDPE	0.51	2000	970
	PE	0.35	2300	920
	PVC	0.15	960	1380
	LDPE	0.34	3400	920
Ground	Clay	1.2	1800	1700
	Sandy	3.12	930	2525
	Sandy-Clay	2.1	1200	1960
	Gravelly Sand	1.7	1860	2800
Working Fluid	Water	0.6	4182	998

2.2 Meshing & Mesh Independence Test

A hybrid meshing technique was adopted for the GHE system and surrounding soil domain. The bulk computational domain was discretized using unstructured tetrahedral elements, while inflation layers were generated around the tube walls to provide finer resolution of the near-wall temperature and velocity gradients. A relatively coarser mesh was used in the regions farther from the GHE to reduce the overall computational cost. The mesh boundaries were designated as inlet, outlet, top, bottom, and surrounding. The finalized mesh used in these numerical simulations is presented in Fig. 2. Furthermore, mesh independence test with three different mesh sizes of 2476565, 6270400, and 7195038 from coarse to fine were tested for the modified GHEs with outlet temperatures stabilized at 298.28 K, 298.27 K, and 298.27 K after 72 hours of operation. With outlet temperature gap of only 0.01 K, the 2,476,565 element mesh was therefore considered sufficiently close to mesh-independent in terms of outlet temperature but relatively coarse meshes inadequately resolve temperature and velocity gradients, wall heat flux, soil-temperature distribution, heat-transfer rate, and pressure drop near the GHE tubes. Fig. 3 illustrates that the outlet temperature initially increased when fewer mesh elements were used, but began to decrease once the mesh size crossed the optimal "convenient point." Therefore, the mesh with 6270400 elements was considered optimal for further investigation.

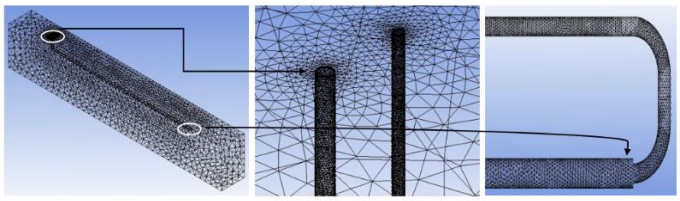

Fig. 2 Numerical mesh of the modified U-tube horizontal GHE

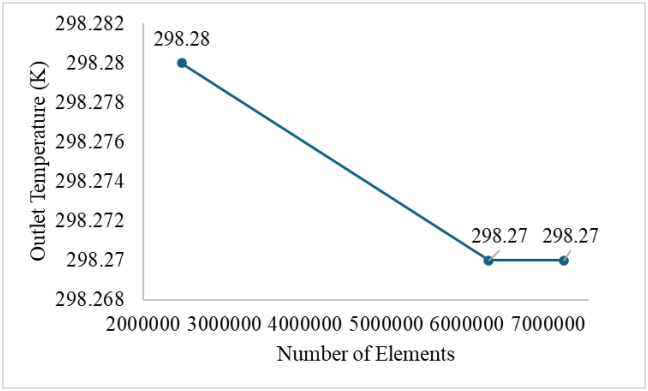

Fig. 3 Mesh independence test of the modified U-tube horizontal GHE

2.3 Simulation Setup and Procedure

Mesh integrity was verified by examining the minimum mesh volume and ensuring no negative values were present, thereby maintaining compliance with the continuity equation. A pressure-based transient solver was utilized due to the incompressible and transient nature of the flow. Gravity was set along the negative Y axis to represent upward gravitational influence, and the energy equation was enabled due to thermal gradients within the system. Based on the Reynolds number (maximum Re=1947), the flow regime was determined to be laminar across all simulations. After specifying the material properties of both pipe and soil, the simulations were executed under cooling mode with the inlet temperature kept at 303 K and the ground temperature initialized at 290 K. The inlet was defined as a mass flow inlet with 2 L/min for the parametric studies to provide a consistent comparison among the investigated configurations, pipe materials and ground material, while the outlet was specified as a pressure outlet. The upper soil surface was assumed to have no heat exchange associated with radiation, convection, or evaporation [18], also the bottom and surrounding boundaries were thermally insulated. Due to the viscous flow through the pipe, the SIMPLE algorithm was employed. The computation was considered converged when the normalized residuals of the governing equations satisfied the specified convergence criterion, with the energy-equation residuals below 10-6. After setting the required parameters, the solution was initialized using the hybrid method, and the equations of energy, continuity, and momentum were solved without any interruption for a duration of 72 hours using a time-step size of 60 s. The 60-s time step was selected to provide sufficient temporal resolution for capturing the transient heat-transfer behavior of the GHE while maintaining a reasonable computational cost for the long-duration simulation.

2.4 Model Validation

The numerical model was validated against the experimental data reported by Yoon et al. [19] for a horizontal U-tube GHE. Minor modifications to the material properties were implemented in the numerical model, while the geometric parameters were maintained identical as reported in the experimental work, comprising HDPE pipes with an inner diameter of 0.016 m and outlet diameter of 0.020 m placed in sand. The pipes were arranged in a U-shaped layout with a spacing of 0.08 m, installed at a depth of 0.5 m, and a total length of 8 m. A mass flow rate of 0.06 kg/s was applied throughout the analysis, and the ground was initialized at a temperature of 290 K. In accordance with the thermal response test (TRT) approach used in Yoon et al.'s [19] experiment, the inlet temperature of the circulating water in the numerical model was allowed to increase with time to reflect the practical difficulty of maintaining a constant inlet temperature under experimental conditions. The simulated heat transfer rate per unit pipe length was 25.90 W/m, which closely matches to the experimental value of 26 W/m, resulting in a deviation of only 0.38%, as shown in Fig. 4. The small discrepancy may be attributed to differences between the numerical assumptions and the experimental conditions. In particular, environmental effects and heat transfer through the soil surface that were not explicitly considered in the numerical model may have contributed to the difference between the predicted and measured heat-transfer rates.

3 Result and Discussion

The thermal performance of modified horizontal U-tube GHE configurations was numerically analyzed to quantify the effect of structural alterations, using indicators such as outlet temperature, heat exchange effectiveness, pressure drop, and temperature contours in cooling mode. The outcomes facilitated

the identification of the most effective configuration and expanded the knowledge of performance variations among the modified horizontal GHE models.

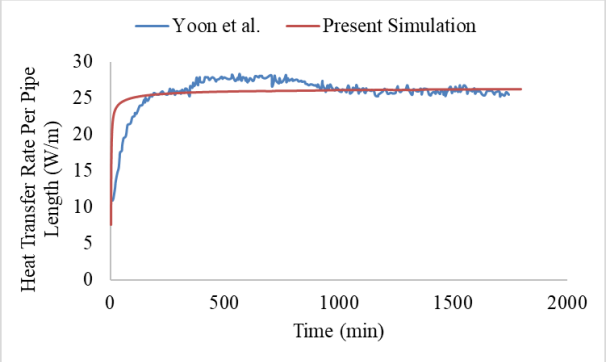

Fig. 4 Numerical Validation of Heat Transfer Rate Per Pipe Length (W/m) vs Time (min)

3.1 Analysis of Outlet Temperature

Thermal performance is assessed by analyzing the temperature difference between the inlet and outlet water. The outlet temperatures recorded after 72 hours of cooling operation demonstrate continuous heat transfer from the fluid to the soil. When the water enters the GHE at a higher temperature than the ground, it gradually loses heat and cools, while the soil surrounding the pipes becomes warmer as it absorbs heat. As illustrated in Fig. 5, the outlet temperature increases sharply at the beginning because the soil is unsaturated and has a high capacity to absorb heat.

Therefore, in the first 24 hours, all models exhibit lower outlet temperatures, indicating efficient thermal exchange between the GHE and the ground. With extended operation, thermal saturation begins to occur in the soil, reducing the temperature gradient between the fluid and the ground. This decline in the thermal driving force leads to a slower heat transfer rate, causing the outlet temperature to rise gradually and resulting in higher temperatures at 72 hours compared to earlier operation times. These results indicate that heat transfer in GHEs is transient in nature and that soil heat accumulation has a noticeable impact on the system's performance over extended periods. Out of the 17 models tested, the C10 and C16 emerged as the most effective, reaching an outlet temperature of 298.27 K after 72 hours, as reported in Table 3.

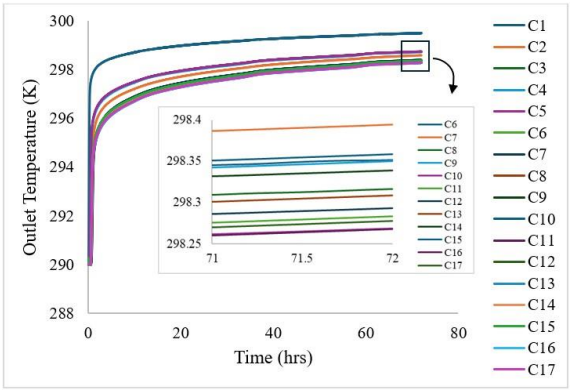

Fig. 5 Outlet Water Temperature Variation with Operational Time

Table 3 Outlet Temperature after 24, 48, and 72 hours of operation

Configurations	Outlet Temperature (K)		
	After 24 h	After 48 h	After 72 h
C1	299.06	299.33	299.50
C2	297.83	298.32	298.58
C3	298.06	298.50	298.74
C4	298.02	298.47	298.71
C5	298.06	298.49	298.74
C6	297.52	298.06	298.35
C7	297.59	298.11	298.39
C8	297.47	298.02	298.32
C9	297.53	298.06	298.35
C10	297.41	297.97	298.27
C11	297.43	297.99	298.28
C12	297.45	298.00	298.29
C13	297.47	298.01	298.31
C14	297.51	298.05	298.34
C15	297.54	298.07	298.36
C16	297.41	297.97	298.27
C17	297.43	297.98	298.28

3.2 Analysis of Heat Transfer Rate

Evaluating the thermal performance of a horizontal GHE involves calculating the heat exchange rate through water flow, as shown in the following equation. The heat transfer rate between the soil and the working fluid stabilizes after 24 hours of operation, which is illustrated in Fig. 6.

$$Q = \dot{m}C_p \Delta T = \dot{m}C_p (T_{in}-T_{out}) \quad (1)$$

Where $\dot{m}$ is the water flow rate, Cp is the specific heat of water, and ΔT is the difference in temperature between the circulating water's inlet and outlet.

The heat transfer rate between the working fluid and soil is initially high due to the substantial temperature difference. The soil was initially maintained at a constant temperature. However, after a few hours, this rate starts to decline as the soil absorbs heat, causing its temperature to gradually approach that of the working fluid. As shown in Fig. 5, the outlet temperatures recorded for cases C10 and C16 were the lowest among all configurations, which explains their comparatively higher heat transfer rates in Fig. 6. Although both perform similarly, C10 shows a slightly higher average heat transfer rate of 700.48 W compared to 700.14 W for C16, offering a minor performance edge. On the other hand, assessing the heat transfer rate per meter of trench provides insight into how effectively the ground is being utilized. A higher W/m value signifies improved spatial efficiency and overall cost-effectiveness of the system. The nearly matching values for C10 of 38.17 W/m and C16 of 38.15 W/m indicate that the operational performances of both cases are almost identical, which is further supported by the results illustrated in Fig. 7.

3.2.1 Effect of Installation Depth

The influence of pipe burial depth on the modified horizontal U-tube GHE was evaluated at depths from 1 m to 2.5 m for C10 with 0.5 m increments. From the graphical representation in Fig. 8, it is evident that the average heat transfer rate rose slightly from 694.64 W to 705.56 W with increasing

depth, reflecting the advantage of stable and moisture-rich soil at lower levels. However, beyond 2 m, the enhancement was less than 0.5%, indicating diminishing efficiency gains.

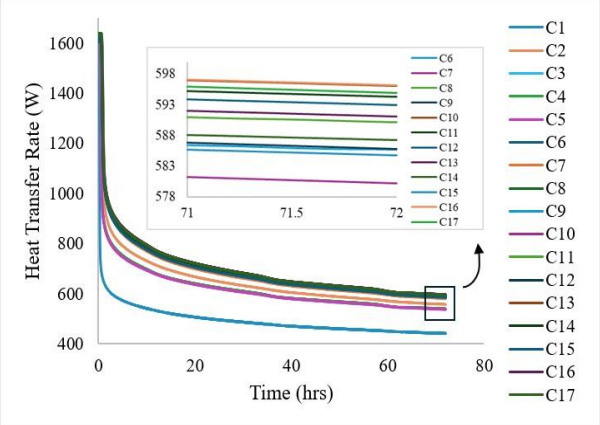

Fig. 6 Heat Exchange Rate Variation with Operational Time

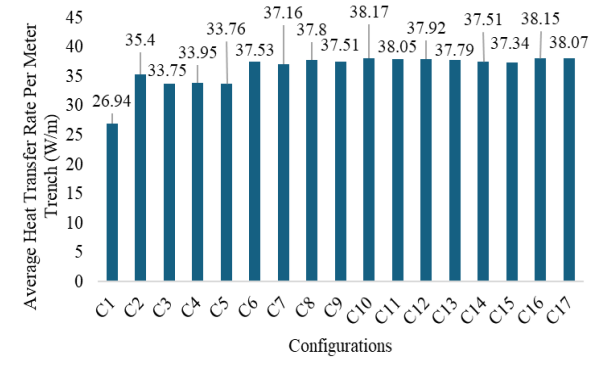

Fig. 7 Variation of Average Heat Exchange Rate Per Meter Trench (W/m)

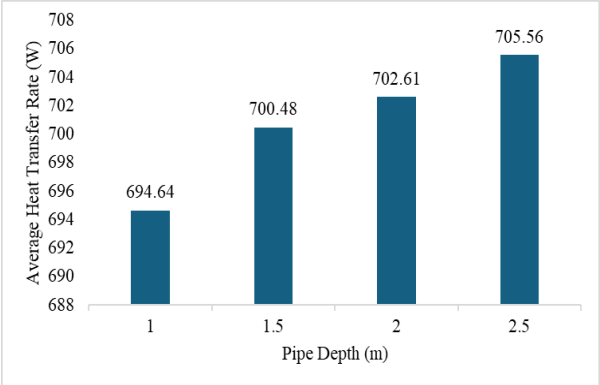

Fig. 8 Heat Exchange Rate Variation with Pipe Depth

3.2.2 Effect of Flow Rate

The effect of flow rate on the thermal performance of the C10 configuration was investigated at 0.5, 1.0, 1.5, and 2.0 L/min. As shown in Fig. 9, the average heat-transfer rate increased from 378.62 W at 0.5 L/min to 565.64 W, 661.99 W, and 700.48 W at 1.0, 1.5, and 2.0 L/min, respectively. Overall, increasing the flow rate from 0.5 to 2.0 L/min enhanced the heat-transfer rate by approximately 85.01%. However, the improvement decreased at higher flow rates, with only a 5.81% increase from 1.5 to 2.0 L/min. Thus, further increasing the flow rate provides a progressively smaller thermal benefit while increasing the pumping requirement.

3.2.3 Effect of Using Different Tube Materials

C10 underwent 72 hours of simulation using various pipe materials ranging from PE to PVC to identify the most efficient one for heat transfer while using clay as the surrounding ground. From the Fig. 10, it is clearly comprehensible that HDPE yielded the highest heat-transfer rate, approximately 16.43% higher than PVC. This difference is mainly associated with the higher thermal conductivity of HDPE (0.51 W/m·K) compared with PVC (0.15 W/m·K).

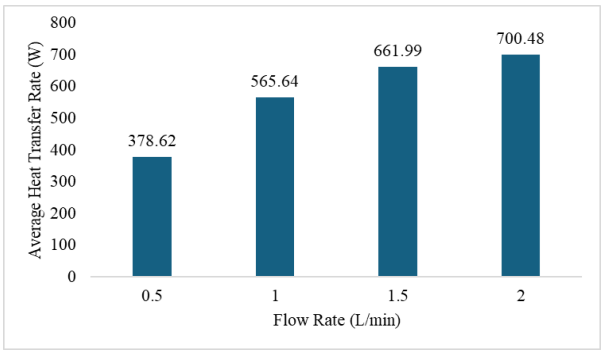

Fig. 9 Heat Exchange Rate Variation with Flow Rate

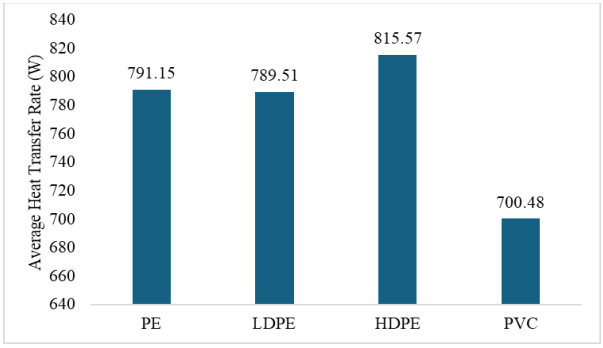

Fig. 10 Heat Exchange Rate Variation with Tube Materials

3.2.4 Effect of Using Different Ground Materials

Sand, clay, sandy-clay, and gravel were selected as ground materials for the simulation studies of C10, while the pipe material was PVC, and other conditions remained constant throughout the analysis. As shown in Fig. 11, the average heat-transfer rates were 892.88 W, 700.48 W, 807.59 W, and 829.56 W for sand, clay, sandy-clay, and gravel, respectively. Sand provided the highest heat-transfer rate, which was approximately 27.47% higher than clay. This difference is mainly associated with the higher thermal conductivity of sand (3.12 W/m·K) compared with clay (1.20 W/m·K), which facilitates heat transfer from the pipe to the surrounding ground.

3.3 Pressure Drop

As the fluid flows through a pipe, it undergoes a pressure drop that is primarily influenced by the design and configuration of the GHE, including pipe length and inner diameter. Therefore, each GHE configuration has a unique pressure drop. For horizontal GHEs, the pressure drop is determined by the pressure difference across the inlet and outlet. The expression for pressure drop is:

$$\Delta P = P_{in} - P_{out} \quad (2)$$

where, ΔP= Pressure drops, P_{in} = Inlet pressure, P_{out} = Outlet pressure

Not only C1 but also C3–C7 exhibit substantial pressure losses, and their heat transfer enhancement remains minimal. This excessive pressure drop can be attributed to longer flow paths or narrower pipe sections, which elevate hydraulic drag rather than improving convective effectiveness. Therefore, these systems tend to consume more energy for circulation with limited heat transfer benefit. On the contrary, C10–C17 experience smaller pressure drops owing to wider tube diameters, which lower frictional effects. These designs seem to optimize both the hydraulic and thermal aspects through proper adjustment of pipe size, surface area, and material volume, ensuring stable flow with sufficient heat exchange efficiency, which is shown in Fig. 12.

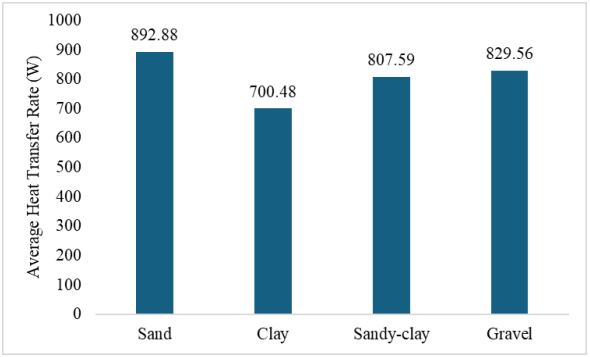

Fig. 11 Heat Exchange Rate Variation with Ground Materials

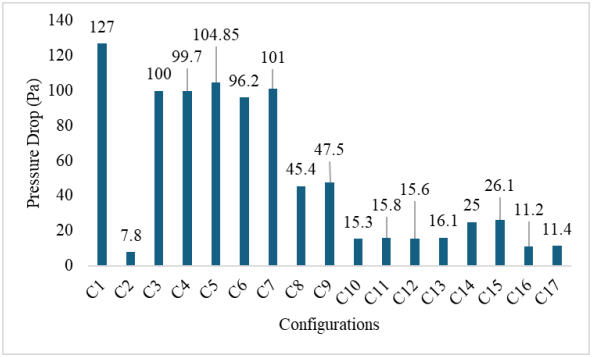

Fig. 12 Comparison of pressure drop in various horizontal GHEs

3.4 Temperature Distribution

The thermal performance of various modified horizontal U-tube GHEs was numerically investigated, showing temperature distribution patterns across the heat exchanger surfaces. This temperature contour analysis provides essential information for optimizing the design of horizontal GHEs to boost cooling performance. A comparison of the contours for modified horizontal GHEs indicated significant variations in their heat exchange capacities.

Fig. 13-Fig. 14 presents three temperature contours of C2, C10, and C16, illustrating the soil's final state with GHE after 72 hours of continuous operation. The uniform diameter of C2 ensures consistent thermal behavior and a moderate heat transfer rate along the pipe, whereas the bottom section exhibits higher heat exchange owing to enhanced ground contact provided by the larger diameter. In contrast, the enlarged outlet sections in C10 and C16 enhance thermal performance by increasing the residence time of the fluid and promoting deeper thermal interaction, which is reflected in the temperature contours showing broader heat diffusion in the lower regions, indicating more effective heat transfer.

Collectively, these observations demonstrate that while C2 ensures consistent thermal behavior, the modifications in C10 and C16 significantly improve energy extraction by optimizing flow dynamics and thermal engagement with the surrounding ground.

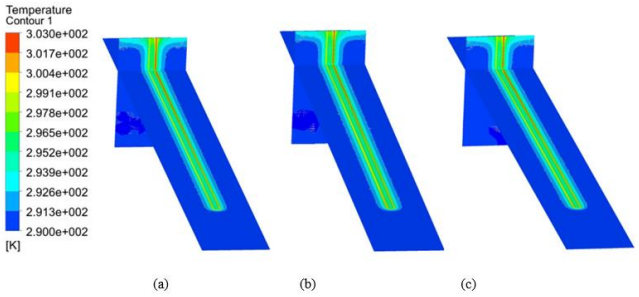

Fig. 13 Contour of Temperature Distribution for (a) C2-left one, (b) C10-middle one, (c) C16-right one (after 72-hour operation)

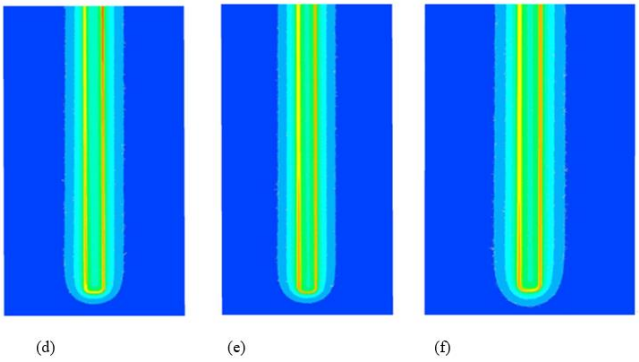

Fig. 14 Temperature distribution Contour of modified section for (a) C2, (b) C10, (c) C16

4 Conclusion

Modified horizontal U-tube GHE configurations have been analyzed to determine their thermal performance, outlet temperature, heat exchange rate, pressure drop, and other factors. Among all tested configurations, C10 and C16 achieved higher thermal performance than the uniform C1 and C2, with average heat transfer rates of 700.48 W and 700.14 W, respectively, compared to 623 W for C1 and 649.58 W for C2 after 72 hours of continuous operation. The highest-pressure loss (127 Pa) was measured in C1 owing to its smaller diameter, whereas C2 recorded the lowest (7.8 Pa) due to its straight geometry with a wider diameter. Modified designs such as C10 and C16 exhibited notably lower pressure drops, minimizing pumping power requirements and improving operational efficiency. The performance of GHEs was strongly influenced by pipe depth, flow rate, material selection, and other factors. Therefore, in this work, optimal results were achieved using HDPE pipes with sand, which provided greater heat transfer efficiency than PE pipes and clay. Since all tests were conducted under continuous 72-hour operation, further research could investigate intermittent cycles or fin integration to expand the heat transfer area and enhance overall thermal performance.

Acknowledgment

We thank Khulna University of Engineering & Technology (KUET), Bangladesh, for logistic support to carry out this work.

Author contribution statement

All authors listed have equally contributed to conceptualization, methodology, data curation, analysis, writing– original draft, review & editing of this article.

Conflict of Interest Statement

The authors declare no conflict of interest.

Funding Statement

The authors did not receive any specific grant from funding agencies in the public, commercial, or not-for-profit sectors.

Generative AI Statement

No generative AI/LLM was used in any stage of this manuscript.

Data Availability

The data that has been used in this study are available within the article.

References

[1] Howarth, J., 2019. When will fossil fuels run out?. *Octopus Energy*.

[2] S. Pandey, "Alternative Sources of Energy: definition, types, benefits & Limitations," Embibe Exams, Jan. 25, 2023. [Online]. Available: https://www.embibe.com/exams/alternative-sources-of-energy/. [Accessed: Aug. 6, 2025].

[3] Rahman, T., Shovon, M.M.A., Sharmin, Z. and Alharbi, T., 2026. Solar and wind energy transition towards a net-zero energy future in Asia: Key factors, drivers, challenges, and future pathways. *Energy Reports*, *15*, p.109353.

[4] Nkinyam, C.M., Ujah, C.O., Asadu, C.O. and Kallon, D.V., 2025. Exploring geothermal energy as a sustainable source of energy: A systemic review. *Unconventional Resources*, *6*, p.100149.

[5] "Renewable Energy Essentials: Geothermal," IEA, 2010. [Online]. Available: https://www.iea.org/reports/renewable-energy-essentials-geothermal. [Accessed: Aug. 6, 2025].

[6] Saleem, A., Ambreen, T. and Ugalde-Loo, C.E., 2024. Energy storage-integrated ground-source heat pumps for heating and cooling applications: A systematic review. *Journal of Energy Storage*, *102*, p.114097.

[7] Ali, M.H., Kariya, K. and Miyara, A., 2017. Performance analysis of slinky horizontal ground heat exchangers for a ground source heat pump system. *Resources*, *6*(4), p.56.

[8] E. Geo, "Difference between horizontal and vertical geothermal ground loops - Envirotech Geothermal," Envirotech Geothermal Ltd., Jun. 05, 2024. [Online]. Available: https://envirotechgeo.com/horizontal-and-vertical-geothermal-ground-loops/. [Accessed: Aug. 6, 2025].

[9] Zou, H., Pei, P., Wang, C. and Hao, D., 2021. A numerical study on heat transfer performances of horizontal ground heat exchangers in ground-source heat pumps. *Plos one*, *16*(5), p.e0250583.

[10] Florides, G. and Kalogirou, S., 2007. Ground heat exchangers—A review of systems, models and applications. *Renewable energy*, *32*(15), pp.2461-2478.

[11] Badescu, V., 2007. Simple and accurate model for the ground heat exchanger of a passive house. *Renewable energy*, *32*(5), pp.845-855.

[12] Benazza, A., Blanco, E., Aichouba, M., Río, J.L. and Laouedj, S., 2011. Numerical investigation of horizontal ground coupled heat exchanger. *Energy Procedia*, *6*, pp.29-35.

[13] Esen, H., Inalli, M. and Esen, M., 2007. Numerical and experimental analysis of a horizontal ground-coupled heat pump system. *Building and environment*, *42*(3), pp.1126-1134.

[14] Adamovsky, D., Neuberger, P. and Adamovsky, R., 2015. Changes in energy and temperature in the ground mass with horizontal heat exchangers—The energy source for heat pumps. *Energy and buildings*, *92*, pp.107-115.

[15] Jahan, N., Ali, M.H. and Miyara, A., 2024. Numerical analysis of thermal performance of various types of horizontal ground heat exchangers. *AIP Advances*, *14*(9).

[16] Hu, L., Rizvi, Z.H., Tobber, L. and Wuttke, F., 2023. Thermal performance of three horizontal ground heat exchanger systems: comparison of linear-loop, spiral-coil and slinky-coil arrangements. *Frontiers in Energy Research*, *11*, p.1188506.

[17] Hossain, M.S., Tutul, M.T.E., Rifat, T.A. and Karim, M., 2023. Parametric Optimization and Efficiency Assessment of Horizontal Earth Water Pipe Heat Exchanger (EWPHE) in the Context of Bangladesh. *Journal of Engineering Science*, *14*(2), pp.79-88.

[18] Hasan, N., Ali, M.H., Pratik, N.A., Lubaba, N. and Miyara, A., 2024. Improving the thermal performance of vertical ground heat exchanger by modifying spiral tube geometry: A numerical study. *Heliyon*, *10*(15).

[19] Yoon, S., Lee, S.R. and Go, G.H., 2015. Evaluation of thermal efficiency in different types of horizontal ground heat exchangers. *Energy and buildings*, *105*, pp.100-105.